

# Photoinduced absorption in disubstituted polyacetylenes: Comparison of theory with experiments

Priya Sony and Alok Shukla

*Physics Department, Indian Institute of Technology, Powai, Mumbai 400076 INDIA*

In a recently performed experiment Korovyanko et al [Phys. Rev. B **67**, 035114 (2003)] have measured the photo-induced absorption (PA) spectrum of phenyl-disubstituted polyacetylenes (PDPA) from  $1B_u$  and  $2A_g$  excited states. In  $1B_u$  PA spectrum they identified two main features namely PA1 and PA2. While in the  $2A_g$  spectrum they identified only one feature called  $PA_g$ . In this paper we present a theoretical study of  $1B_u$  and  $2A_g$  PA spectra of oligo-PDPA's using correlated-electron Pariser-Parr-Pople (P-P-P) model and various configuration interaction (CI) methodologies. We compare the calculated spectra with the experiments, as well as with the calculated spectra of polyenes of the same conjugation lengths. Calculated spectra are in good agreement with the experiments. Based upon our calculations, we identify PA1 as the  $mA_g$  state and  $PA_g$  as the  $nB_u$  state of the polymer. Regarding the PA2 feature, we present our speculations. Additionally, it is argued that the nature of excited states contributing to the  $2A_g$ -PA spectra of oligo-PDPA's is qualitatively different from those contributing to the spectra of polyenes.

PACS numbers: 78.30.Jw, 78.20.Bh, 42.65.-k

## I. INTRODUCTION

Recently discovered class of conjugated polymers called phenyl-disubstituted polyacetylenes (PDPA's)—obtained by substituting the side H atoms of *trans*-polyacetylene by phenyl derivatives—have exhibited very interesting optical properties.<sup>1,2,3,4,5,6,7,8</sup> Despite their structural similarities to *trans*-polyacetylene—which is well-known to be nonphotoluminescent—PDPA's are known to exhibit photoluminescence (PL) with large quantum efficiency.<sup>5</sup> We explained this apparently contradictory behavior, in our earlier papers,<sup>9,10,11</sup> in terms of reduced electron-correlation effects caused by the delocalization of exciton in the transverse direction because of the presence of phenyl rings. It was argued in those papers that because of the reduced correlation effects, the first two-photon excited state  $2A_g$  state is higher in energy than the first one-photon excited state  $1B_u$  state in PDPA's, rendering these materials photoluminescent.<sup>9,10,11</sup> This ordering of excited states is exactly opposite to that in *trans*-polyacetylene, where relatively stronger correlation effects shift the  $2A_g$  state lower than the  $1B_u$  state, making the material weakly emissive.<sup>12,13</sup> Furthermore, we argued that in PDPA's, the delocalization of excitons has couple of more important consequences on their optical properties: (a) reduced optical gaps as compared to *trans*-polyacetylene, and (b) significant presence of transverse polarization in the photons emitted during the PL in PDPA's, a prediction, which since then, has been verified in several experiments.<sup>8,14</sup>

Recently, Korovyanko *et al.*<sup>15</sup> have probed the excited states of PDPA's using the photoinduced absorption (PA) spectroscopy, leading to measurement of excited states so far unexplored in linear optics. They measured the PA spectrum of oligo-PDPA's both from the  $1B_u$  as well as  $2A_g$  excited states. Using the dipole selection rules for centro-symmetric polymers such as PDPA's, it is obvious that the PA spectrum from the  $1B_u$  state will have peaks corresponding to the higher  $A_g$ -type states, while those in the  $2A_g$  spectrum will have features corresponding to higher  $B_u$ -type states. In the PA spectrum from the  $1B_u$  state, Korovyanko et al. report observing two prominent features, referred as PA1 and PA2 by them.<sup>15</sup> While in the PA spectrum from the  $2A_g$  state, they observed only one feature which they called the  $PA_g$  peak.<sup>15</sup> To understand the nature of the excited states leading to these PA peaks, however, one needs to perform detailed theoretical calculations of the PA spectra of oligo-PDPA's of various sizes, and compare the theoretical results to the experimental ones. Since, it is well-known that the electron-correlation effects play very important roles in proper description of the excited states of conjugated polymers,<sup>12,13</sup> the calculations must properly take them into account. Studying these excited states will also enlighten us about the nonlinear optical properties of PDPA's because some of these excited states will also be visible in their nonlinear spectra, such as two-photon absorption (TPA), and third-harmonic generation (THG). It is with this aim in mind that we have undertaken a systematic theoretical study of the PA spectra of oligo-PDPA's of varying sizes. In the present work, we have used the Pariser-Parr-Pople (P-P-P) model Hamiltonian and employed a configuration-interaction (CI) method based approach to perform the correlated calculations of the low-lying excited states, and the PA spectra, of this material. We also compare the states visible in the PA spectra of PDPA's with those in their TPA and the THG spectra computed by us recently.<sup>16,17</sup>

The remainder of this paper is organized as follows. In section II we briefly describe the theoretical methodology used to perform the calculations in the present work. Next in section III we present and discuss the calculated PA

SHUKLA–SONY: Fig 1

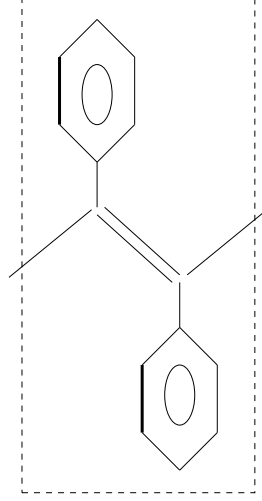


Figure 1: The unit cell of PDPA. The phenyl rings are rotated with respect to the  $y$ -axis, which is transverse to the axis of the polyene backbone ( $x$ -axis)

spectra of oligo-PDPA's. Finally, in section IV we summarize our conclusions.

## II. THEORY

The unit cell of PDPA oligomers considered in this work is presented in Fig. 1. To the best of our knowledge, the geometry of PDPA's in the ground state, is still not known. However, it is intuitively clear that the steric hindrance would cause a rotation of the substituent phenyl rings so that they would no longer be coplanar with the backbone of the polymer. The extent of this rotation is also unknown; however, it is clear that the angle of rotation will be less than 90 degrees because that would effectively disconnect the phenyl rings from the backbone. In our previous works<sup>9,10,11</sup>, we argued that the steric hindrance effects can be taken into account by assuming that the phenyl rings of the unit cell are rotated with respect to the  $y$ -axis by 30 degrees in such a manner that the oligomers still have inversion symmetry. It is obvious that along the direction of conjugation ( $x$ -direction), PDPA is structurally similar to *trans*-polyacetylene, with alternating single and double bonds. In the following, we will adopt the notation PDPA- $n$  to denote a PDPA oligomer containing  $n$  unit cells of the type depicted in Fig. 1.

The point group symmetry of *trans*-polyacetylene and polyenes is  $C_{2h}$  so that the one-photon states belong to the irreducible representation (irrep)  $B_u$ , while the ground state and the two-photon excited states belong to the irrep  $A_g$ . Because of the phenyl group rotation mentioned above, the point group symmetry of PDPA's and its oligomers is  $C_i$  so that its ground state and the two-photon excited states belong to the irreps  $A_g$  and  $A_u$ , respectively. However, to keep the comparison with *trans*-polyacetylene transparent, we will refer to them as  $A_g$  and  $B_u$  irreps.

The correlated calculations on the oligomers PDPA- $n$  were performed using the P-P-P model Hamiltonian

$$H = H_C + H_P + H_{CP} + H_{ee}; \quad (1)$$

where  $H_C$  and  $H_P$  are the one-electron Hamiltonians for the carbon atoms located on *trans*-polyacetylene backbone (chain), and the phenyl groups, respectively,  $H_{CP}$  is the one-electron hopping between the chain and the phenyl units and  $H_{ee}$  depicts the electron-electron repulsion. The individual terms can now be written as,

$$H_C = \sum_{hk, jk^0, i, jM} (t_0 - (-1)^M t) B_{kj, k^0, jM, jM+1}; \quad (2a)$$

$$H_P = \sum_{h; i, jM} t_0 B_{h; jM, jM}; \quad (2b)$$

and

$$H_{CP} = \sum_{hk; i; M} t_{\tau} B_{k; M; i; M} \quad (2c)$$

$$H_{ee} = U \sum_i n_i n_{i\#} + \frac{1}{2} \sum_{i \neq j} V_{ij} (n_i - 1) (n_j - 1) \quad (3)$$

In the equation above,  $k, k^0$  are carbon atoms on the polyene backbone,  $i, j$  are carbon atoms located on the phenyl groups, while  $i$  and  $j$  represent all the atoms of the oligomer.  $M$  is a unit consisting of a phenyl group and a polyene carbon,  $h$  implies nearest neighbors, and  $B_{ij; M; M^0} = (C_{i; M}^y; C_{j; M^0}^y; + h.c.)$ . Matrix elements  $t_0$ , and  $t_{\tau}$  depict one-electron hops. In  $H_C$ ,  $t$  is the bond alternation parameter arising due to electron-phonon coupling. In  $H_{CP}$ , the sum over  $i$  is restricted to atoms of the phenyl groups that are directly bonded to backbone carbon atoms. There is a strong possibility that due to the closeness of the phenyl rings in the adjacent unit cells, there will be nonzero hopping between them, giving rise to a term  $H_{PP}$  in the Hamiltonian above. However, in our earlier study,<sup>10</sup> we explored the influence of this coupling on the linear optics of these materials, and found it to have negligible influence. Therefore, in the present study, we are ignoring the phenyl-phenyl coupling.

As far as the values of the hopping matrix elements are concerned, we took  $t_0 = 2.4$  eV, while it is imperative to take a smaller value for  $t_{\tau}$ , because of the twist in the corresponding bond owing to the steric hindrance mentioned above. We concluded that for a phenyl group rotation of 30 degrees, the maximum possible value of  $t_{\tau}$  can be 1.4 eV.<sup>9</sup> Bond alternation parameter  $t = 0.168$  eV chosen for the backbone was consistent with the value usually chosen in the P-P-P model calculations performed on polyenes.

The Coulomb interactions are parameterized according to the Ohno relationship<sup>18</sup>,

$$V_{ij} = U = \epsilon_{ij} (1 + 0.6117 R_{ij}^2)^{-1/2}, \quad (4)$$

where,  $\epsilon_{ij}$  depicts the dielectric constant of the system which can simulate the effects of screening,  $U$  is the on-site repulsion term, and  $R_{ij}$  is the distance in Å between the  $i$ th carbon and the  $j$ th carbon. The Ohno parameterization initially was carried out for small molecules, and, therefore, it is possible that the Coulomb parameters for the polymeric samples could be somewhat smaller due to interchain screening effects.<sup>19</sup> In various calculations performed on phenylene-based conjugated polymers including PDPA's<sup>9,10,11,16,17,20,21</sup>, we have noticed that "screened parameters" with  $U = 8.0$  eV and  $\epsilon_{ii} = 1.0$ , and  $\epsilon_{ij} = 2.0$ , otherwise, proposed by Chandross and Mazumdar<sup>19</sup>, lead to much better agreement with the experiments, as compared to the "standard parameters" with  $U = 11.13$  and  $\epsilon_{ij} = 1.0$ , proposed originally by Ohno. Therefore, in the present work we compare the results of our "screened parameter" based calculations with the experiments, while the results of our "standard parameter" based calculations are compared with similar calculations performed on corresponding polyenes. This is mainly because screened parameters are not suitable for polyenes. Moreover, comparison between oligo-PDPA's and polyenes, based upon calculations performed with the same set of PPP parameters, will help us appreciate the influence of phenyl substitution on the properties of PDPA's.

In all the calculations, C-C bond length of 1.4 Å was used for the phenyl rings. In polyenes and PDPA's, along the backbone the single bonds and the double bonds were taken to be 1.45 Å and 1.35 Å, respectively. The bond connecting the backbone to the substituent phenyl rings was taken to be 1.40 Å.

The starting point of the correlated calculations for various oligomers were the restricted Hartree-Fock (HF) calculations, using the P-P-P Hamiltonian. The many-body effects beyond HF were computed using different levels of the configuration interaction (CI) method, namely, quadruples-CI (QCI), and the multi-reference singles-doubles CI (MRSDCI). Details of these CI-based many-body procedures have been presented in our earlier works.<sup>10,16,17,20</sup>

Since the number of electrons in oligo-PDPA's is quite large because of the large unit cell, it is not possible to include all the orbitals in the correlated calculations. Therefore, it is imperative to reduce the number of degrees of freedom by removing some orbitals from the many-body calculations. In order to achieve that, for each oligomer we first decided as to which occupied and the virtual orbitals will be active in the many-body calculations based upon: (a) their single-particle HF energies with respect to the location of the Fermi level, and (b) charge distribution of various orbitals with respect to the chain/phenylene-based atoms, which was quantified by contribution of the chain-based carbon atoms to the normalization of a given orbital. Because of the particle-hole symmetry in the problem, the numbers of active occupied and virtual orbitals were taken to be identical to each other, with the occupied and virtual

orbitals being particle-hole symmetric. The inactive occupied orbitals were held frozen during the CI calculations, while the inactive virtual orbitals were simply deleted from the list of orbitals. When we present the CI results on various oligo-PDPA's, we will also identify the list of active orbitals. From the CI calculations, we obtain the eigenfunctions and eigenvalues corresponding to the correlated ground and excited states of various oligomers. Using the many-body wave functions, we compute the matrix elements of the dipole operator amongst different states and use them, along with the energies of the excited states, to compute various PA spectra.

### III. RESULTS AND DISCUSSION

In this section we will first briefly discuss the main features of the experimental PA spectrum obtained by Korovyanko *et al.*,<sup>15</sup> and then present and discuss the theoretical results obtained in our calculations.

#### A. Experimental Results

First we briefly review the quantitative aspects of the experimental results of Korovyanko *et al.*<sup>15</sup> who measured the PA spectra of PDPA from  $1B_u$  and  $2A_g$  excited states. In  $1B_u$  PA spectrum they identified two PA bands, the first one of which was at 1.1 eV called PA1, and the second one at 2.0 eV referred to as PA2. In the  $2A_g$  spectrum they identified only one PA band called  $PA_g$  located at 1.7 eV. By dipole selection rules it is clear that the states leading to peaks in  $1B_u$  spectrum will be of  $A_g$  type, while those in the  $2A_g$  spectrum will be of  $B_u$  type.

Another aspect of the PA spectra that we will keep in mind while comparing the theory to the experimental data, is its connection to nonlinear optical properties. For example, it is well known that nonlinear optical properties of conjugated polymers are determined by a small number of excited states namely  $1B_u$ ,  $m A_g$ , and  $n B_u$ .<sup>12,13</sup> Here  $m A_g$  is an excited state which has large dipole coupling to the  $1B_u$  state and is visible in TPA and THG spectra, while  $n B_u$  is a state with large dipole coupling to the  $m A_g$  state, and is visible in the THG spectra of conjugated polymers.<sup>12,13</sup> Thus it is obvious that the  $m A_g$  state should contribute significantly to the  $1B_u$  PA spectra. Whether  $n B_u$  will contribute to the  $2A_g$  PA spectrum will depend on, whether or not, it has a large dipole coupling with the  $2A_g$  state. In a recent theoretical analysis of the  $1B_u$  PA spectra of PPV which also has two prominent bands labeled PA1 and PA2, we indeed found that the first and the most intense peak (PA1) contributing to the spectra was indeed the  $m A_g$  state of the polymer.<sup>21</sup>

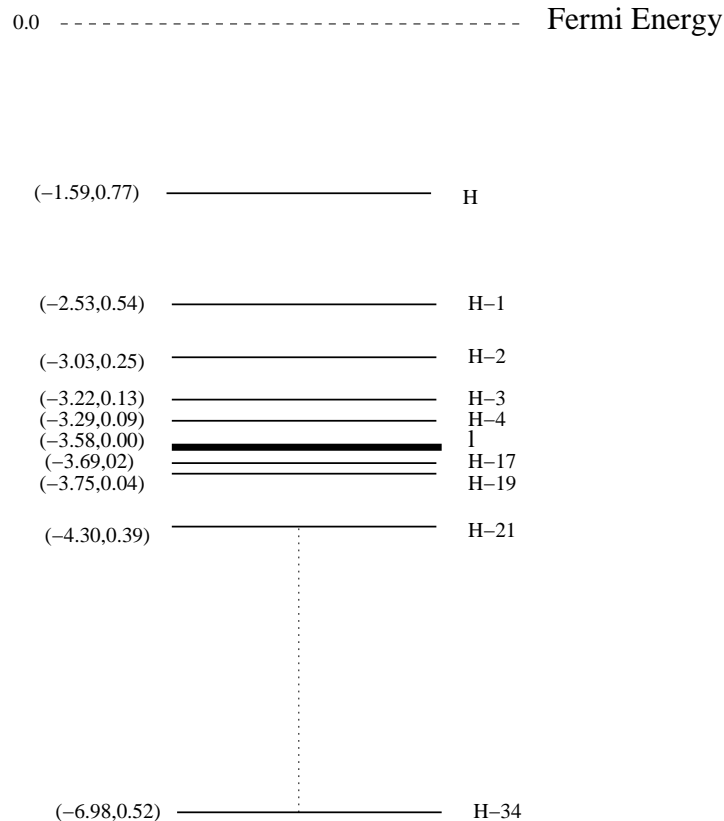
#### B. Theoretical Results

We have performed correlated calculations of the PA spectrum of oligomers PDPA-5 and PDPA-10. The reasons behind choosing these oligomers is that the conjugation lengths of the oligomers under experimental conditions is believed to be short.<sup>14</sup> Resonant Raman scattering based studies in films of PDPA-nBu have indicated that the mean conjugation length is seven repeat units,<sup>8</sup> while in the solution phase it is believed to be close to five repeat units.<sup>14</sup> Therefore, we believe that our choice of the oligomers PDPA-5 and PDPA-10 is well-suited for comparisons with experiments.

Before presenting our results, we would like to briefly describe the type of correlated calculations performed, and the approximations involved. The correlated calculations performed were of two types: (a) QCI and (b) MRSDCI. Given the large number of electrons in these systems (fourteen electrons/cell), QCI or the MRSDCI methods are not feasible for them if all the orbitals of the system are retained in the calculations. Since it is intuitively clear that the low-lying excited states of the system will be determined by orbitals closest to the Fermi level which have large charge distribution of backbone carbon atoms, in the QCI calculations we decided to include only these orbitals. Therefore, for PDPA-n we included n occupied, and n virtual orbitals closest to the Fermi level in the QCI calculations. Remaining occupied orbitals were frozen and virtual orbitals were deleted as explained in section II. The charge distribution of these n orbitals is as follows: HOMO/LUMO ( $H=L$  for short) orbitals have the largest charge distribution on the chain-based atoms with this quantity decreasing monotonically for  $H=L+i$  orbitals with increasing  $i$  ( $i < n$ ). Levels located next are  $n-1$  orbitals which have zero contribution from the chain atoms, followed by other orbitals. The orbital energy diagram for PDPA-5 is presented in Fig. 2. The computational effort associated with the QCI calculations on PDPA-n is, therefore, same as that needed for a polyene with n double bonds. Although for PDPA-10, it leads to Hilbert space dimensions in excess of one million, however, using the approach reported in our earlier works<sup>10,20</sup>, we managed to obtain low-lying excited states for this set of calculations. We do believe that, despite the orbital truncation, the QCI calculations should describe the lowest of the excited states reasonably well.

Figure 2: The occupied energy levels of PDPA-5 obtained from the Hartree-Fock calculations performed using the screened parameters. As indicated, the Fermi energy has been shifted to zero. On the left of each level there are two numbers, first of which is the energy of the level in eV, and the second one is the charge distribution of the orbital quantified as the contribution of chain carbon atoms to the orbital normalization. Contribution of the carbon atoms on the phenyl rings, to the orbital charge distribution can be obtained by subtracting this number from one. On the right of each level is the location of the level with respect to the HOMO (H). The thick line indicated as 1 represents the band composed of localized orbitals of the phenyl rings. Because of the particle-hole symmetry of the half-filled PPP model, virtual levels will be mirror symmetric with respect to the Fermi level. Additionally, virtual orbital  $L + i$  will have the same charge distribution as the occupied orbital  $H - i$ .

## Shukla–Sony: Fig. 2

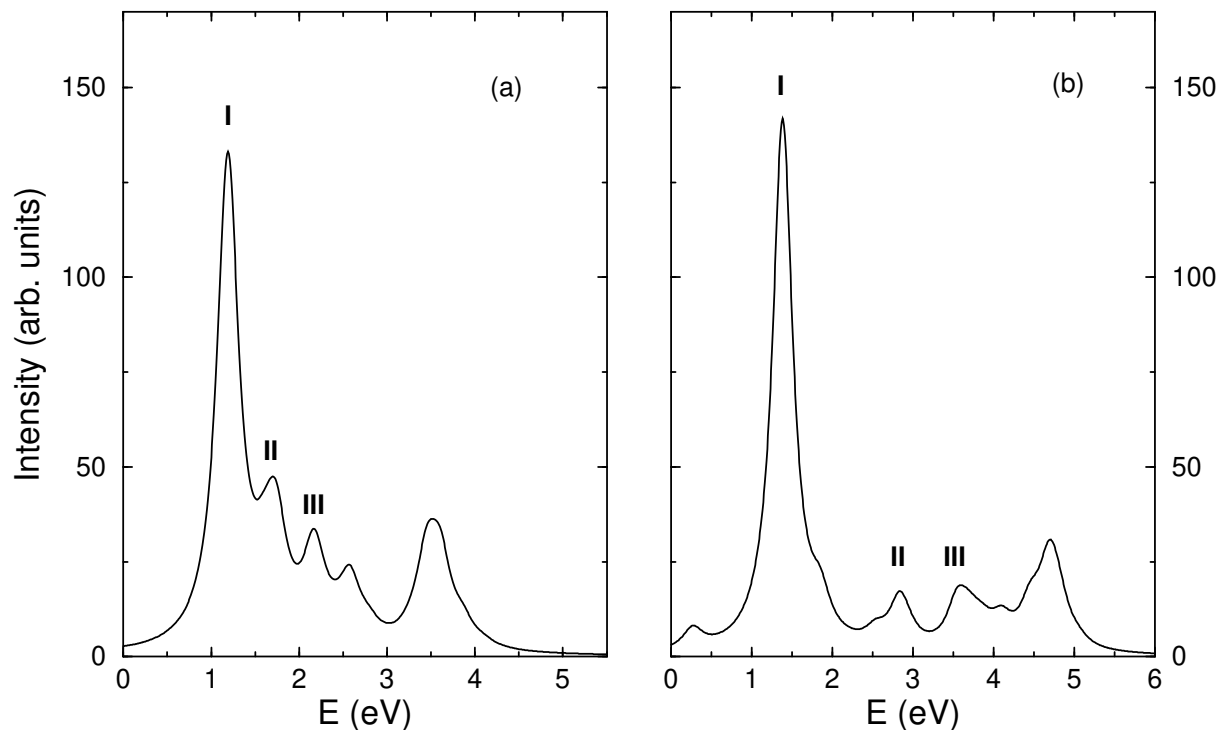


In order to improve upon the aforesaid orbital truncation scheme, we augmented the orbital set by including orbitals with large charge distribution on the phenylene-based carbon atoms. Phenylene-based orbitals are of two-types: (a) delocalized orbitals ( $d=d$ ) with significant population on all six phenyl-based carbon atoms and (b) localized orbitals ( $l=l$ ) with nonzero population only on four phenyl-based carbon atoms. It is intuitively clear that  $l=l$  type orbitals will participate more in the excitations localized on the phenyl rings, because these orbitals will have negligible population on the phenyl-based carbon atom connected to the back bone (cf. Fig. 1). On the other hand  $d=d$  orbitals in PDPA's will be involved in excitations extending from backbone to the phenyl rings. Since it is these type of excitations which are next in energy, we augmented the orbital set by also including the phenyl-based  $d=d$  orbitals. However, with this augmented orbital set, only MRSDCI calculations are feasible, and those too on oligomers with comparatively smaller conjugation length. But, given the small conjugation lengths in the experimental samples discussed above, we believe that this is not a severe limitation. Thus, these MRSDCI calculations were performed on PDPA-5 using thirty orbitals (15 occupied + 15 virtual) in all, ten of which were chain-based orbitals closest to the Fermi level (also included in the QCI calculations mentioned above), while remaining twenty were from the  $d=d$  phenyl-based orbital set mentioned above. In the MRSDCI calculations, we used 25 reference configurations for the  $A_g$ -type states, and 24 for the  $B_u$ -type states leading to CI matrices of dimensions close to half-a-million both for the  $A_g$  and  $B_u$  manifolds.

Thus, to summarize, we present QCI calculations performed on PDPA-5 and PDPA-10 utilizing restricted orbital

Figure 3: PA spectrum of PDPA-5 from its  $1B_u$  state, computed using: (a) MRSDCI method, and (b) QCI method. First three peaks have been labeled and discussed in the text. A linewidth of 0.15 eV was assumed.

Shukla–Sony Fig 3



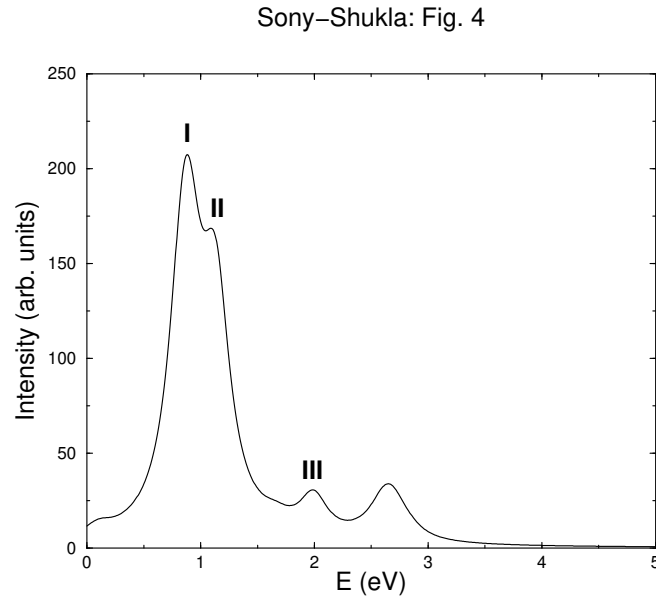
sets, and MRSDCI calculations on PDPA-5 utilizing an augmented orbital set. QCI calculations were performed with orbitals closest to the Fermi level, several of which had large charge distribution on carbon atoms based on the backbone. MRSDCI calculations were performed with an orbital set which, in addition to the orbitals used in the QCI calculations, also contained  $d=d$  with large charges on the carbon atoms based on phenyl rings. Thus, the results of QCI and MRSDCI calculations should be in good agreement with each other for those excited states, which can be described mainly in terms of orbitals based on backbone atoms. While the excited states in which electrons get significantly delocalized onto the phenyl rings, will be described better by MRSDCI calculations. Thus, by comparing the results of these two types of calculations for PDPA-5 with each other, we can assess as to where the results of the two approaches begin to diverge from each other. This will also let us form an opinion about the results obtained for PDPA-10, for which no MRSDCI results are available. It is with this information about the uncertainties associated with various calculations, we present our theoretical results and compare them to the experimental ones, in the next section.

### 1. $1B_u$ PA Spectrum

The spectrum from  $1B_u$  excited state of PDPA-5 calculated using QCI and MRSDCI methods, and the screened parameters, is shown in Fig. 3. For PDPA-10 the same spectrum computed using the QCI method is given in Fig. 4. In Tables I and II we present energies and wave functions of the excited states, contributing to the spectra of Figures 3 and 4. Before discussing the spectra in detail, we identify their broad features. It is clear from the figures that each spectrum starts with a very intense peak followed by a number of weaker features. Upon comparing the calculated intensity profile with the experimental one,<sup>15</sup> we find general agreement between the two. However, in the experimental spectrum the intensity of feature PA2 is not as drastically smaller compared to PA1 as in case of theoretical spectrum.

Upon examining the theoretical results with experimental feature PA1 in mind, in both the MRSDCI and QCI

Figure 4: PA spectrum of PDPA-10 from its  $1B_u$  state, computed using the QCI method. Only the peaks in the experimental energy region have been labeled. A linewidth of 0.15 eV was assumed.



spectra corresponding to PDPA-5, only one excited state contributes to the first feature. In PDPA-10 spectrum, the first absorption band has one intense peak (I) followed by a closely spaced shoulder (II), contributions to which come from three rather closely spaced excited states. Thus for PDPA-10 (Fig. 4), we interpret both I and II as part of the same peak, to be compared to the experimental band PA1. Upon examining the many-particle wave functions of the excited states contributing to the first peak in various calculations (tables I and II) we conclude that the configurations contributing to them are essentially identical in all the cases. Since this conclusion is based upon calculations of various types (QCI, MRSDCI), and on different oligomers (PDPA-5, PDPA-10), we conclude that these results are universally valid for PDPA's. Comparing these states to ones contributing resonant peaks of the TPA and THG spectra of oligo-PDPA's calculated by us earlier<sup>16,17</sup>, we conclude that these states correspond to nothing but the  $m A_g$  states of the corresponding oligo-PDPA. Recalling that  $m A_g$  is the state with a very strong dipole coupling to the  $1B_u$  state which makes its presence prominent in both the TPA and THG spectra of several conjugated polymers,<sup>13,21</sup> it should not at all be surprising that it leads to an intense peak in their  $1B_u$  PA spectrum as well. Indeed, in a recent calculation performed on oligomers of PPP and PPV,<sup>21</sup> we identified the first feature of their  $1B_u$  PA spectra with their  $m A_g$  states. Upon examining the dipole coupling of  $m A_g$  states of oligo-PDPA's to their  $1B_u$  states, we find: (a) this to be mainly directed along the longitudinal direction, and (b) that in terms of magnitude the coupling of this state to the  $1B_u$  state to be the largest among all other  $A_g$  type excited states.

Regarding the quantitative aspects of our calculations, it is obvious from table I that for PDPA-5, the peak position of PA1 obtained from the QCI calculations (1.38 eV) is in good agreement (within 0.2 eV) of the one computed from the MRSDCI calculation (1.19 eV). This result is consistent with the fact that for PDPA-5, wave functions of the states contributing to PA1 obtained from QCI and MRSDCI calculations are in excellent agreement with each other, and consist mainly of excitations close to the Fermi level (cf. table I). The calculated peak positions of PA1 for various oligomers are presented in table V, along with the corresponding experimental value. We note that results of MRSDCI calculation for PDPA-5 (1.19 eV) appear to be in the best agreement with the experiments (1.1—1.2 eV).

For features beyond PA1 for PDPA-5, the results of QCI and MRSDCI calculations begin to diverge from each other both for the wave functions of the excited states, as also their peak positions. As far as experimental feature PA2 (at 2.0 eV) is concerned, we find that none of the peaks in the QCI spectrum of PDPA-5 are close to that. However, in the MRSDCI spectrum of PDPA-5, feature II located at 1.72 eV, and feature III located at 2.17 eV, could be considered as possible candidates. Upon examining the MRSDCI wave functions of PDPA-5 in table I of states  $6A_g$  (peak II) and  $9A_g$  (peak III), we find that they predominantly consist of singly excited configurations. In case of peak II, these singly excited configurations have almost equal contributions from low-lying excitations as well as high-lying excitations, involving chain and phenylene based delocalized orbitals. However, state  $9A_g$  (peak III) mainly consists of singly excited high-lying configurations among the chain based orbitals and the phenylene based orbitals. Looking at the polarization of the photons involved, the computed dipole connecting the  $1B_u$  state to states  $6A_g$

Table I: Excited states contributing to the  $1B_u$  PA spectrum of PDPA-5 computed using the QCI and the MRSDCI methods corresponding to the spectra of Fig. 3. The heading Wave Function lists the most important configurations contributing to the many-body wave function, and their coefficients, as per our adopted notation.<sup>22</sup>

Method	Peak	State	Peak Position (eV)	Wave Function
QCI	I	$4A_g (m A_g)$	1.38	$\mathcal{H} ! L + 1i + c\mathbf{x}:(0.37)$ $\mathcal{H} ! L;H ! Li(0.74)$
MRSDCI	I	$4A_g (m A_g)$	1.19	$\mathcal{H} ! L + 1i + c\mathbf{x}:(0.41)$ $\mathcal{H} ! L;H ! Li(0.58)$
QCI	II	$9A_g$	2.83	$\mathcal{H} ! L + 1;H \quad 1 ! Li + (0.47)$ $\mathcal{H} ! L;H ! Li + c\mathbf{x}:(0.36)$ $\mathcal{H} ! L;H \quad 4 ! Li + c\mathbf{x}:(0.22)$ $H ! L;H \quad 2 ! Li + c\mathbf{x}:(0.21)$
MRSDCI	II	$6A_g$	1.72	$\mathcal{H} ! L + 19i + c\mathbf{x}:(0.38)$ $\mathcal{H} \quad 2 ! L + 1i + c\mathbf{x}:(0.30)$ $\mathcal{H} ! L + 17i + c\mathbf{x}:(0.26)$
QCI	III	$12A_g$	3.56	$\mathcal{H} ! L + 1;H \quad 1 ! Li + c\mathbf{x}:(0.51)$ $\mathcal{H} ! L;H \quad 2 ! Li + c\mathbf{x}:(0.38)$ $\mathcal{H} ! L;H \quad 3 ! Li + c\mathbf{x}:(0.32)$
MRSDCI	III	$9A_g$	2.17	$\mathcal{H} ! L + 21i + c\mathbf{x}:(0.57)$ $\mathcal{H} ! L;H ! Li(0.18)$

Table II: Excited states contributing to the  $1B_u$  PA spectrum of PDPA-10, computed using the QCI method, and presented in Fig. 4. Rest of the information is same as given in the caption of table I.

Peak	State	Peak Position (eV)	Wave Function
I	$3A_g (m A_g)$	0.81	$\mathcal{H} ! L;H ! Li(0.37)$ $\mathcal{H} ! L + 3i + c\mathbf{x}:(0.31)$ $\mathcal{H} ! L + 1i + c\mathbf{x}:(0.29)$
	$4A_g (m A_g)$	0.87	$\mathcal{H} ! L + 1;H ! L + 1i + c\mathbf{x}:(0.29)$ $ H ! L + 3i + c\mathbf{x}:(0.42)$ $\mathcal{H} ! L + 1i + c\mathbf{x}:(0.27)$ $\mathcal{H} ! L;H ! Li(0.33)$ $\mathcal{H} \quad 1 ! L;H ! L + 1i(0.31)$ $\mathcal{H} ! L;H ! L + 2i + c\mathbf{x}:(0.21)$
II	$5A_g (m A_g)$	1.12	$\mathcal{H} ! L;H ! Li(0.38)$ $\mathcal{H} \quad 1 ! L;H ! L + 1i(0.33)$ $\mathcal{H} ! L;H ! L + 2i + c\mathbf{x}:(0.29)$ $\mathcal{H} \quad 1 ! L + 2i + c\mathbf{x}:(0.26)$ $\mathcal{H} ! L + 1i + c\mathbf{x}:(0.20)$
III	$11A_g$	1.99	$\mathcal{H} ! L;H \quad 2 ! L + 2i(0.30)$ $\mathcal{H} ! L + 3;H \quad 1 ! Li + c\mathbf{x}:(0.21)$ $\mathcal{H} \quad 2 ! L + 3i + c\mathbf{x}:(0.26)$

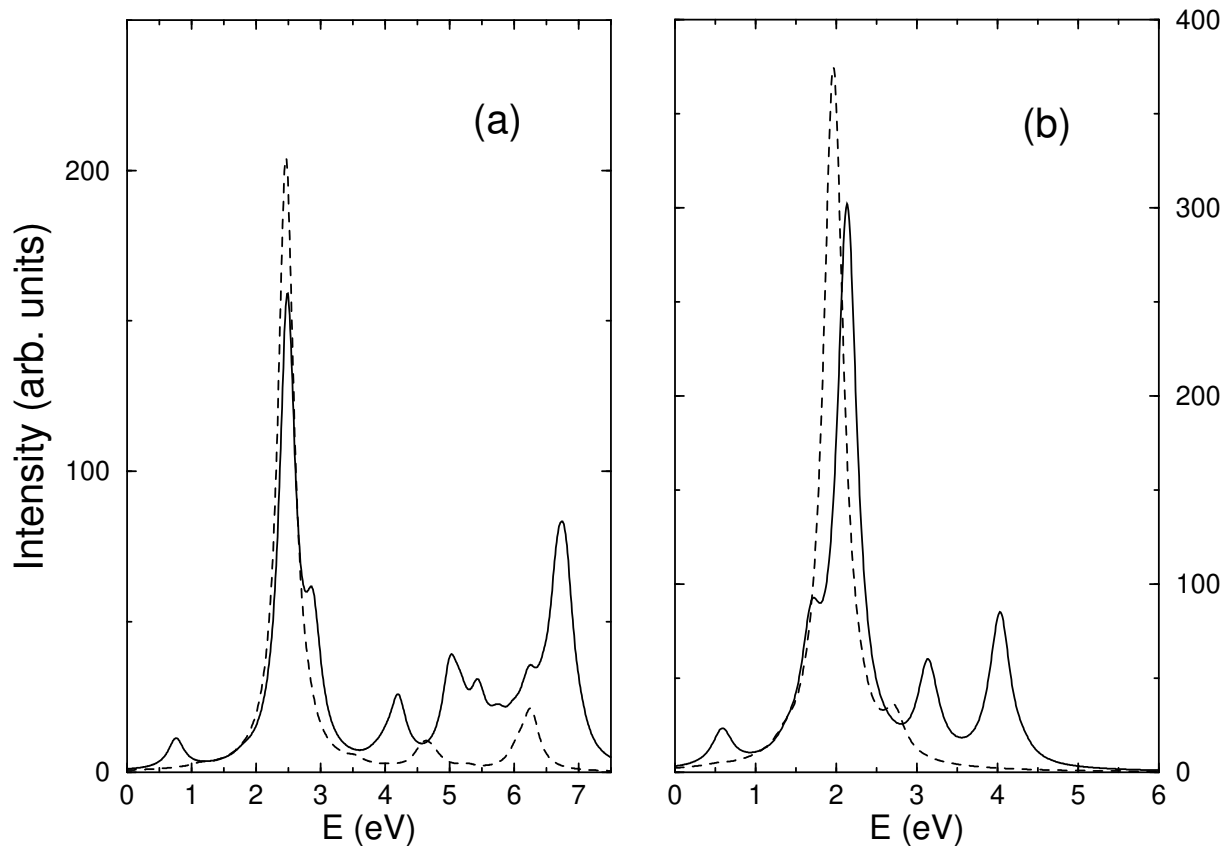
suggests mixed polarization, with  $y$  component (transverse) being more intense. The corresponding dipole moment connecting  $1B_u$  state to the  $9A_g$  state, on the other hand, suggests mainly an  $x$  polarized (longitudinal) transition.

In the QCI spectrum of PDPA-10, feature III which is located exactly at 2.0 eV is can also be considered a very good candidate for PA2. The many particle wave function of the state involved ( $11A_g$  in table II) is a mixture of higher energy singly and doubly excited configurations. As far as transition dipoles are concerned, we find it to be an almost equal mixture of  $x$  and  $y$  components. Thus, as far as the polarization of the photon, and the nature of excited states involved in the feature PA2 we have a disagreement between our MRSDCI results on PDPA-5, and QCI results on PDPA-10. In order to resolve this issue, it will be of interest to perform experiments on oriented samples, and measure the polarization of the photons contributing to the feature PA2.



Figure 5: Comparison of  $1B_u$  PA spectra of oligo-PDPA's with polyenes of the same conjugation length: (a) spectra of PDPA-5 (solid line) and five double-bond polyene (dashed line), and (b) spectra of PDPA-10 (solid line) and ten double-bond polyene (dashed line). All the spectra were computed using the QCI method and the standard parameters in the PPP Hamiltonian. For PDPA- $n$ , QCI calculations were performed with  $n$  occupied/virtual orbitals closest to Fermi level. A common linewidth of 0.15 eV was used to compute the spectra.

Sony-Shukla: Fig. 5



Next we compare the  $1B_u$  PA spectra of oligo-PDPA's with those of corresponding polyenes. Both for polyenes and the PDPA's, we use the standard parameters in the PPP Hamiltonian, coupled with the QCI method. Thus, calculations on oligo-PDPA's were performed with a restricted set of orbitals as explained earlier, while for polyenes all the orbitals were used. The results of our calculations are presented in Fig. 5. The peak positions for both PDPA-5 and PDPA-10 are blue shifted as compared to those computed with the screened parameters. For example, the position of the first peak for PDPA-5 with standard parameters is 2.5 eV, as compared to 1.38 eV obtained with the screened parameters and the 1.2 eV experimental value. Thus, quantitatively speaking, the PA spectra of oligo-PDPA's computed using the standard parameters are not in good agreement with the experimental results. From Fig. 5 we also conclude that the first peak of both oligo-PDPA's and the corresponding polyenes are both due to the  $m A_g$  states of the system concerned. This lends further credence to our earlier conclusion that  $m A_g$  state of oligo-PDPA's, which corresponds to the PA1 feature of the experimental spectrum, is mainly due to chain-based excitations. Also from Fig. 5 it is obvious that, unlike oligo-PDPA's, in the polyene PA spectra there is no significant structure beyond the first peak. This is in excellent agreement with our earlier conclusion that the experimental feature PA2 is mainly due to the excitations involving phenylene-based orbitals.

Figure 6: PA spectrum of PDPA-5 from its  $2A_g$  excited state, computed using: (a) MRSDCI method, and (b) QCI method. A linewidth of 0.15 eV was assumed. Feature I corresponds to the  $PA_g$  feature of the experiment.<sup>15</sup> Additionally, we have labeled and discussed (see text) the next peak (feature II) of the spectra, with the possibility of it being detected in future experiments.

Shukla–Sony Fig. 6

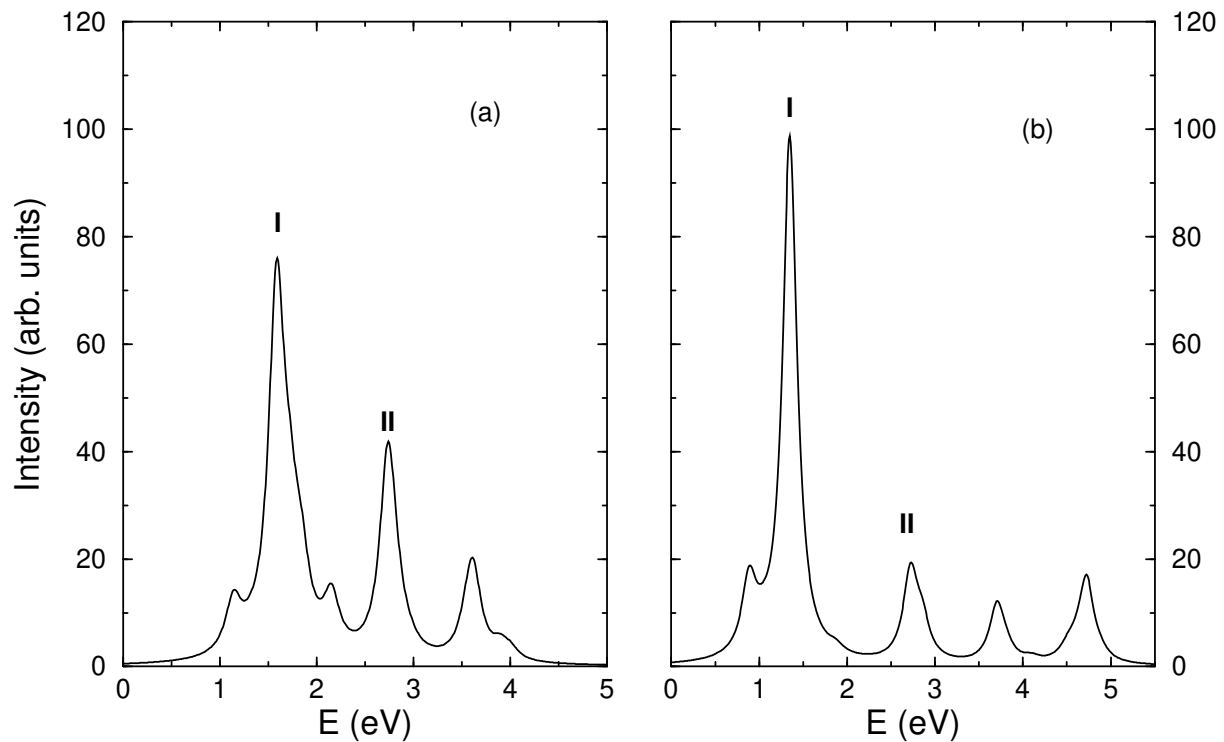


Figure 7: PA spectrum of PDPA-10 from its  $2A_g$  excited state, computed using the QCI method. Only the peaks in the experimental region have been labeled. A linewidth of 0.15 eV was assumed.

Sony–Shukla: Fig. 7

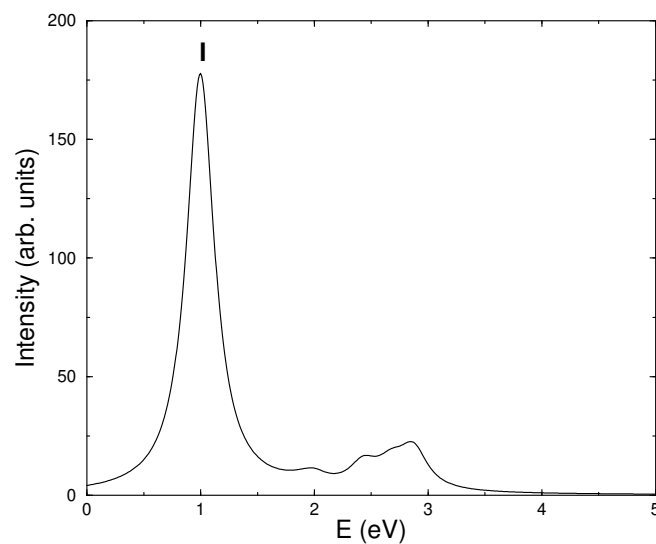


Table III: Excited states contributing to the  $2A_g$  PA spectrum of PDPA-5 computed using the QCI and MRSDCI methods, and presented in Fig. 6. Rest of the information is same as given in table I.

Method	Peak	State	Peak Energy (eV)	Wave Function
QCI	I	$4B_u (nB_u)$	1.35	$\frac{1}{\sqrt{2}} (H_{-1} - L_{+1})$ $\frac{1}{\sqrt{2}} (H_{-1} - L_{+1} + c_{\pi}(0.14))$
MRSDCI	I	$4B_u (nB_u)$	1.59	$\frac{1}{\sqrt{2}} (H_{-1} - L_{+1})$ $\frac{1}{\sqrt{2}} (H_{-16} - L_{+1} + c_{\pi}(0.15))$ $\frac{1}{\sqrt{2}} (H_{-1} - L_{+1} + c_{\pi}(0.13))$
QCI	II	$9B_u (kB_u)$	2.73	$\frac{1}{\sqrt{2}} (H_{-1} - L_{+1} + c_{\pi}(0.57))$ $\frac{1}{\sqrt{2}} (H_{-1} - L_{+1} + c_{\pi}(0.25))$ $\frac{1}{\sqrt{2}} (H_{-1} - L_{+1})$
MRSDCI	II	$9B_u (kB_u)$	2.74	$\frac{1}{\sqrt{2}} (H_{-1} - L_{+1} + c_{\pi}(0.48))$ $\frac{1}{\sqrt{2}} (H_{-1} - L_{+1} + c_{\pi}(0.27))$ $\frac{1}{\sqrt{2}} (H_{-4} - L_{+4})$

## 2. $2A_g$ PA spectrum

The PA spectra from the  $2A_g$  excited state of PDPA-5 computed using the screened parameters, at the MRSDCI and QCI levels, are shown in Fig. 6, while that for PDPA-10 computed at the QCI level is presented in Fig. 7. The peak positions and the wave functions of the many-body states for these spectra are listed in tables III and IV. It is clear from the theoretical  $PA_g$  spectra that the intensity is dominated by just one peak (peak I) with smaller contributions from a series of weak peaks. This aspect of theoretical spectrum is in excellent agreement with the experiment which reports only one peak.<sup>15</sup> We identify peak I in all the computed spectra as the  $nB_u$  state of the polymer. The same  $nB_u$  state had also contributed significantly to the longitudinal THG spectra of these oligomers as reported in our earlier work.<sup>17</sup> The  $nB_u$  state reported here has a significantly strong  $y$ -polarized dipole coupling to the  $1A_g$  ground state. However, it has a much stronger  $x$ -polarized dipole coupling to the  $2A_g$  state. Therefore, in experiments performed on oriented samples, we predict the  $PA_g$  feature of oligo-PDPA's to be mainly due to  $x$ -polarized photons leading to an absorption from the  $2A_g$  state to the  $nB_u$  state. In case of conjugated polymers such as *trans*-polyacetylene, PPV, and PPP etc.,<sup>13,21</sup> the  $nB_u$  state has strong dipole coupling to the  $mA_g$  state. However, in PDPA's the state we have identified as  $nB_u$  has a very strong dipole coupling with the  $2A_g$  state, and a comparatively weaker coupling to the  $mA_g$  state. The state with large dipole coupling to the  $mA_g$  state contributes to the computed THG spectrum of PDPA's, and was identified earlier by us as the  $kB_u$  state.<sup>17</sup>

As far as the many-particle wave function of the state  $nB_u$  corresponding to the  $PA_g$  feature is concerned, we have excellent agreement among various calculations performed on different oligomers. From tables III and IV it is obvious that this state mainly consists of singly excited configuration among orbitals  $H_{-1}$  and  $L_{+1}$ . Regarding the calculated peak positions of  $PA_g$ , for PDPA-5 the MRSDCI value (1.59 eV) differs from the QCI value (1.35 eV) by 0.24 eV. Thus, the disagreements between the results of QCI and MRSDCI calculations for PDPA-5 both for  $PA_1$  (0.20 eV) and  $PA_g$  (0.24 eV) are almost similar in size. The only difference between the MRSDCI and the QCI for PDPA-5 spectra is regarding the intensity, and, quite expectedly, the nature of the states contributing to peaks beyond  $PA_g$  in the spectra. For example, in Fig. 6, peak II in the MRSDCI spectrum of PDPA-5 has considerably larger intensity as compared to the same peak in the QCI spectrum. Peak II corresponds to the  $kB_u$  state for the case of PDPA-5 and has been discussed earlier.<sup>17</sup> The character of the  $kB_u$  state as computed in the MRSDCI calculations differs somewhat from that computed in the QCI calculations in that MRSDCI  $kB_u$  state has significant contribution from the singly excited configurations involving phenyl based orbitals. However, both the MRSDCI and QCI calculations predict the  $2A_g \rightarrow kB_u$  optical transition to be mainly  $y$ -polarized. Thus, if future experiments on oriented samples are able to probe features beyond  $PA_g$  in the  $2A_g$ -PA spectrum of oligo-PDPA's, the results of our calculations can be tested.

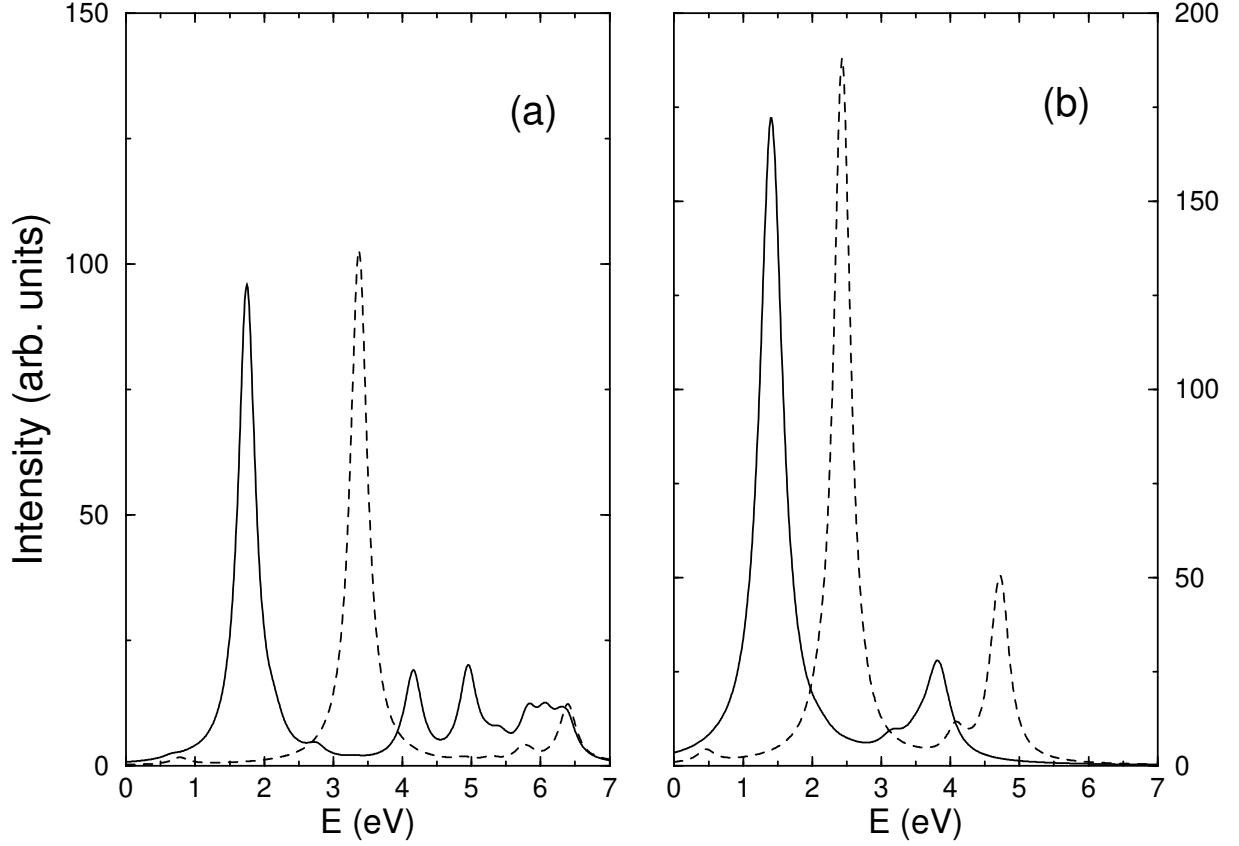
Next we compare the  $2A_g$ -PA spectra of oligo-PDPA's with polyenes as presented in Fig. 8. The spectra presented were computed using the QCI approach, and the standard parameters in the PPP Hamiltonian, for all the oligomers. The peak positions in the oligo-PDPA spectra in this figure are blue shifted as compared those computed with the screened parameters. For example, the locations of the first peaks in the PDPA-5/PDPA-10 spectra are at 1.74/1.41 eV, as compared to their screened parameter locations of 1.35/1.00 eV. This suggests that the same trends will also hold for more sophisticated MRSDCI calculations, thus taking them outside the range of the experimental location of  $PA_g$ . As far as comparison of the  $2A_g$ -PA spectra of oligo-PDPA's and polyenes is concerned, the shapes of the spectra of the two materials look qualitatively similar, although quantitatively speaking PDPA spectra are extremely

Table IV: Excited state contributing to the  $2A_g$  PA spectrum of PDPA-10, computed using the QCI method, and presented in Fig. 7. Rest of the information is same as given in table I.

Peak	State	Peak Energy (eV)	Wave Function
I	$3B_u$ ( $nB_u$ )	1.00	$\Psi = 1 \cdot L + 1i(0.72)$ $\Psi = L + 2i + c\pi(0.38)$ $\Psi = L; H = 1 \cdot L + c\pi(0.14)$

Figure 8:  $2A_g$ -PA spectra of (a) PDPA-5 (solid line) and five double-bond polyene (dashed line), and (b) PDPA-10 (solid line) and ten double-bond polyene (dashed line). Rest of the information is same as in the caption of Fig. 5.

Sony–Shukla: Fig 8



redshifted as compared to their polyene counterparts. However, upon closer examination, we find that the nature of the excited states contributing the first peaks in these spectra are completely different in polyenes as compared to oligo-PDPA's. Going by the definition of the  $nB_u$  state as the one which leads to a strong peak in the THG spectrum,<sup>13</sup> we have identified the first and the most intense peak of oligo-PDPA  $2A_g$  spectrum as the  $nB_u$  state. However, the first and the most intense peak of the calculated  $2A_g$ -PA spectra of polyenes is not due to the  $nB_u$  state, but rather due to a state which is considerably lower in energy than the  $nB_u$  state, and is invisible in the THG spectra. For example, for the five double-bond polyene the first peak is due to the  $3B_u$  state located at 6.79 eV, while the  $nB_u$  state for that polyene is located at 9.25 eV, with respect to the ground state. Similarly, for the ten double-bond polyene the first peak is again due to its  $3B_u$  state located at 5.50 eV, while the  $nB_u$  state is at 7.14 eV. This peculiar aspect of the  $2A_g$ -PA spectra of polyenes will be discussed elsewhere in detail.<sup>23</sup> However, here we would like to emphasize that in the  $2A_g$ -PA spectra of oligo-PDPA's, the  $nB_u$  has a strong presence, while in that of polyenes another lower energy  $B_u$  state contributes to the spectra with large intensity, while the  $nB_u$  state is essentially invisible.

Table V: Summary of theoretical results, and their comparison to the experimental values,<sup>15</sup> where possible. For polarization directions, x implies along the chain, while y implies perpendicular to it. For calculations where more than one states were possible candidates for an experimental feature (see text), information is provided for all of them. Mean conjugation length of the oligomers in experiments is believed to be five to seven repeat units.

Oligomer	Method	Peak Position (Theory)	Polarization (Theory)	Peak position (Exp.)
PDPA-5	QCI	1.38 eV ( $m A_g$ )	mainly x	1.1–1.2 eV (PA1)
PDPA-5	MRSDCI	1.19 eV ( $m A_g$ )	mainly x	
PDPA-10	QCI	0.81–1.12 eV ( $m A_g$ )	mainly x	
PDPA-5	QCI	2.83 eV	mixed	2.0 eV (PA2)
PDPA-5	MRSDCI	1.72–2.17 eV	mixed(larger y)/mainly x	
PDPA-10	QCI	1.99 eV	mixed	
PDPA-5	QCI	1.35 eV ( $n B_u$ )	mainly x	1.7 eV ( $PA_g$ )
PDPA-5	MRSDCI	1.59 eV ( $n B_u$ )	mainly x	
PDPA-10	QCI	1.00 eV ( $n B_u$ )	mainly x	

#### IV. SUMMARY AND CONCLUSIONS

In conclusion, we presented correlated calculations of PA spectra of oligo-PDPA's, and compared our theoretical results to the recent experimental results of Korovyanko *et al.*<sup>15</sup> Good qualitative agreement was obtained between the calculated spectra, and the measured ones, for oligomers. As far as the specific aspects of the spectra are concerned, PA1 feature of the  $1B_u$  PA spectrum, and the  $PA_g$  feature of the  $2A_g$  PA spectrum have been unambiguously identified as the  $m A_g$  and  $n B_u$  states of the polymer, respectively. In both the cases, the polarization of the photons involved in the transition have been predicted to be mainly along the conjugation direction. Our confidence regarding these predictions stems from the fact that various calculations performed on both PDPA-5 and PDPA-10 were all in excellent agreement with each other as far as the nature of the many-particle wave functions of these states, and the polarizations of the photons are concerned. The only peak regarding which our predictions at present are somewhat uncertain is the PA2 feature of the  $1B_u$  PA spectrum. Our MRSDCI calculations on PDPA-5, identified it with excited states whose wave functions consist of significant contributions from the chain-based orbitals close to the Fermi level to the high-lying phenylene-based  $d=d$  orbitals.

Regarding the quantitative aspects, we summarize the results of all our calculations, and their comparison to experiments, in table V. From the table it is clear that overall, the results of MRSDCI calculations performed on PDPA-5 are in very good quantitative agreement with the experimental results as far as the peak positions are concerned. Combined with the assertion by the experimentalists that most of the oligomers are five to seven repeat units long,<sup>8,14</sup> one is tempted to believe that the present theory describes the experimental situation quite well. But, we believe that such speculations are immature until the time the experimental results are also available on the polarizations of the photons involved in the transitions leading to various peaks. Therefore, it will be extremely helpful if future experiments are performed on oriented samples so that the polarizations of the photons involved in the transition can be measured, and the theory presented here is tested more stringently.

#### Acknowledgments

This work was supported by grant no. SP/S2/M-10/2000 from Department of Science and Technology (DST), Government of India.

- 
- <sup>1</sup> K. Tada, R. Hidayat, M. Hirohata, M. Teraguchi, T. Masuda and K. Yoshino, Jpn. J. Appl. Phys., part 2 **35**, L1138 (1996).  
<sup>2</sup> K. Tada, R. Hidayat, M. Hirohata, H. Kajii, S. Tatsuhara, A. Fujii, M. Ozaki, M. Teraguchi, T. Masuda and K. Yoshino, Proc. SPIE-Int. Soc. Opt. Eng., **3145**, 171 (1997).  
<sup>3</sup> M. Liess, I. Gontia, T. Masuda, K. Yoshino, and Z.V. Vardeny, Proc. SPIE-Int. Soc. Opt. Eng., **3145**, 179 (1997).  
<sup>4</sup> A. Fujii, M. Shkunov, Z.V. Vardeny, K. Tada, K. Yoshino, M. Teraguchi and T. Masuda, Proc. SPIE-Int. Soc. Opt. Eng., **3145**, 533 (1997).  
<sup>5</sup> I. Gontia, S.V. Frolov, M. Liess, E. Ehrenfreund, Z.V. Vardeny, K. Tada, H. Kajii, R. Hidayat, A. Fujii, K. Yoshino, M. Teraguchi and T. Masuda, Phys. Rev. Lett. **82**, 4058 (1999).

- <sup>6</sup> R. Sun, Y. Wang, X. Zou, M. Fahlam, Q. Zheng, T. Kobayashi, T. Masuda and A.J. Epstein, Proc. SPIE-Int. Soc. Opt. Eng., **3476**, 332 (1998).
- <sup>7</sup> R. Hidayat, S. Tatsuhara, D.W. Kim, M. Ozaki, K. Yoshino, M. Teraguchi and T. Masuda, Phys. Rev. B **61**, 10167 (2000).
- <sup>8</sup> A. Fujii, R. Hidayat, T. Sonoda, T. Fujisawa, M. Ozaki, Z.V. Vardeny, M. Teraguchi, T. Masuda, and K. Yoshino, Synth. Met. **116**, 95 (2001).
- <sup>9</sup> A. Shukla and S. Mazumdar, Phys. Rev. Lett **83**, 3944 (1999).
- <sup>10</sup> H. Ghosh, A. Shukla, and S. Mazumdar, Phys. Rev. B **62**, 12763 (2000).
- <sup>11</sup> A. Shukla, H. Ghosh, and S. Mazumdar, Synth. Met. **116**, 87 (2001).
- <sup>12</sup> S.N. Dixit, D. Guo, and S. Mazumdar, Phys. Rev. B **43**, 6781 (1991).
- <sup>13</sup> S. Mazumdar and F. Guo, J. Chem. Phys. **100**, 1665 (1994).
- <sup>14</sup> I.I. Gontia, Z.V. Vardeny, T. Masuda, and K. Yoshino, Phys. Rev. B **66**, 075215 (2002).
- <sup>15</sup> O. J. Korovyanko, I. I. Gontia, Z. V. Vardeny, T. Masuda, and K. Yoshino, Phys. Rev. B **67**, 035114 (2003).
- <sup>16</sup> A. Shukla, Chem. Phys. **300**, 177 (2004)
- <sup>17</sup> A. Shukla, Phys. Rev. B **69**, 165218 (2004).
- <sup>18</sup> K. Ohno, Theor. Chim. Acta **2**, 219 (1964).
- <sup>19</sup> M. Chandross and S. Mazumdar, Phys. Rev. B **55**, 1497 (1997).
- <sup>20</sup> A. Shukla, Phys. Rev. B **65**, 125204 (2002).
- <sup>21</sup> A. Shukla, H. Ghosh, and S. Mazumdar, Phys. Rev. B **67**, 245203 (2003).
- <sup>22</sup> The many-particle wave functions of half-filled conjugated polymers such as PDPA exhibit particle-hole (charge conjugation) symmetry when treated using the models such as the Hubbard model and the PPP model. Therefore, for every configuration which contributes to its wave function, its charge-conjugated (c.c.) counterpart will contribute in equal measure. For example, if configuration  $\mathcal{H} \rightarrow L + 1i$  occurs in the wave function with coefficient 0.69, configuration  $\mathcal{H} \rightarrow L - 1i$  will also occur in the wave function with coefficient of the same magnitude (although, the sign could be reversed). Thus, we will use shorthand notation  $\mathcal{H} \rightarrow L + 1i + c.c. (0.69)$  to denote the contribution of these configurations to the wave function. Above,  $H = L$  refer to HOMO/LUMO orbitals.
- <sup>23</sup> A. Shukla and S. Mazumdar, in preparation.